



Control loop test - "from prototype to mass production"

L. Selzer*, B. Bust, J. Morich, S. Odenbach

Professorship for Magnetofluid Dynamics, Measurement and Automation Technology, Institute for Mechatronic Mechanical Engineering, Faculty of Mechanical Engineering, TU Dresden

Abstract

Aufgrund der Restriktion von Präsenzveranstaltungen ab dem Sommersemester 2020 sind die Praktika der Vorlesung „Mess- und Automatisierungstechnik“ von Laborversuchen, die am Lehrstuhl durchgeführt wurden, hin zu Heimversuchen überarbeitet worden, die von zu Hause aus absolviert werden können. Bei der ersten Generation von Praktikumsversuchen dieser Art wurde auf eine Voll- oder Teildigitalisierung von ursprünglichen Versuchen, sowie der Neuentwicklung von Versuchen gesetzt, wobei gängige Alltagsmaterialien für die Versuche verwendet wurden, um den Materialaufwand von Seiten des Lehrstuhls zu minimieren. In der zweiten Generation sollte ein Materialpaket erstellt werden, welches in der Form eines Experimentierkoffers für die Durchführung vom Lehrstuhl ausgeliehen wird. Der Regelkreisversuch stellt einen dieser „Koffer-Versuche“ dar und hat die Anwendung, Einstellung sowie Charakterisierung verschiedener Regler zum Inhalt. Die Entwicklung des Regelkreisversuches, sowie eine detaillierte Durchführung des Versuchs sollen in diesem Beitrag erläutert werden.

Due to restrictions in face-to-face teaching with the summer semester of 2020, the practical courses of the lecture "measurement and automation technology" got restructured from lab courses being performed at the institute to "at home" courses, which can be done by the students from their own home. In the first generation, existing courses received a full or partial digitalization and new courses were developed, which used everyday items. All these courses did not require any materials provided by the institute. For the second generation of "at home" courses a material bundle was designed, which students could borrow from the institute in the shape of a suitcase. The control loop course is one of these suitcase courses and encompasses the application, tuning and characterization of various control loops. The development of the control loop course, as well as a detailed testing of the course are part of this article.

*Corresponding author: Lukas.Selzer@tu-dresden.de

1. The initial situation

At the Chair of Magnetofluid Dynamics, Measurement and Automation Technology, due to the restrictions of classroom lectures for the summer semester 2020, practical experiments of the lecture "Measurement and Automation Technology" (MAT) were changed into home experiment variants, whenever this was possible with relatively little material resources. This was done either by using materials that can be found in the student environment, such as a smartphone camera for an experiment in digital image processing, or by completely digitizing experiments that had a high digital content in the original version, such as measurement dynamics [1]. However, for the summer semester 2021, practical experiments ought to be developed in which the materials are provided in the form of an experimental kit that can be borrowed from the chair and returned after completion of the practical course. Since it was also necessary to take into account those who could not do so due to their social situation, for example because they were no longer in the immediate vicinity, a do-it-yourself variant was also developed at the same time. The people concerned had to buy the necessary materials themselves and were thus still able to carry out the experiments. The basis of the experiments was the use of Arduino microcontrollers. The control loop experiment represents an experiment that was revised for this purpose and whose redevelopment will now be described in more detail below.

2. The original control loop test

First, the original control loop experiment will be described. This represents one of the first practical experiments developed at the chair and deals with PID controllers, their settings and the behavior of the system with different controller parameters. The experiment is made of a Plexiglas pipe (plant) into which water is pumped from a bucket via a submersible pump. The water level (controlled variable x) is determined by a pressure gauge and the output of the submersible pump (manipulated variable z) is controlled by a regulator according to the setpoint. The original setup is shown in Fig. 1 shown.

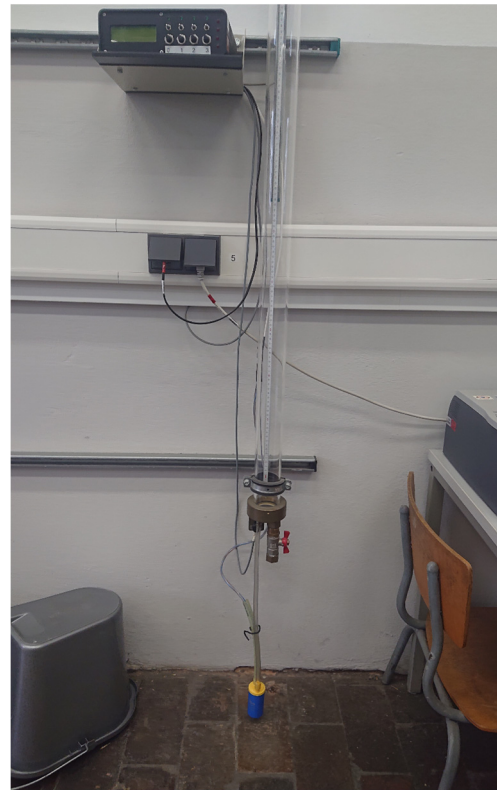


Fig. 1: Original control loop test with plexiglass pipe, submersible pump, valve and the controller box.

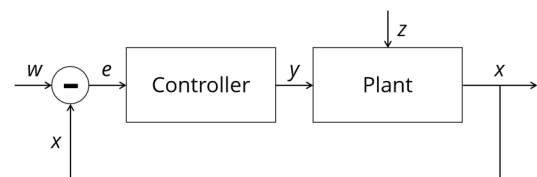


Fig. 2: Schematic representation of a control loop with the setpoint w , the controlled variable x , the control deviation e , the manipulated variable y and the disturbance variable z .

A schematic of a control loop is shown in Fig. 2. A great deal of this experiment is focused on the evaluation of the system responses for given controller parameters, but not on the various methods of determining the parameters themselves. The controller therefore remains a kind of "black box" in which the parameters are entered. Due to the large pipe diameter, the setup is also relatively slow, resulting in long execution times.

3. The first prototype

The new experimental setup was supposed to fit into a suitcase if possible, to have a faster performance and to allow a higher level of interaction with the controller itself. The first

prototype was made of a high-temperature pipe (plant), with the fan of a hair dryer at the lower end of the pipe, and a Styrofoam ball inside the pipe. Two cardboard boxes were used to hold the setup. An Arduino was used to measure the ball distance (d , controlled variable x) from the upper end of the pipe to the upper side of the Styrofoam ball by an ultrasonic sensor and the power of the fan was controlled by pulse width modulation (PWM , controlled variable y) accordingly. The set distance could be varied by a potentiometer. For the PID controller, the open-source library "Arduino PID Library" by Brett Beauregard was used, which covers the required functionalities [2]. Since the ball distance is measured and decreases with higher power of the fan, the PID controller is used in an inverse mode.



Fig. 3: Components of the first prototype consisting of a high-temperature pipe, a hairdryer fan, a Styrofoam ball, an Arduino and an ultrasonic sensor. The breadboard simplifies the wiring of all components. A 3D-printed socket is used to attach the fan to the pipe.

The change of medium from water aimed to significantly reduce the execution times, but also changed the physical relationships of the controlled variable and the manipulated variable. In the case of the water pipe, the pressure increases linearly with the water level and the power required by the pump. This linear relationship of controlled and manipulated variable is important for a PID controller. In the case of the air pipe, on the other hand, the pressure is constant along the length of the pipe, so that for the polystyrene ball with the buoyancy force F_A and the gravitational force F_G there are three cases to be considered:

- $F_A < F_G$: the ball falls
- $F_A = F_G$: the ball remains in its position
- $F_A > F_G$: the ball rises

However, this non-linear relationship between ball distance and motor power can be avoided by making holes in the high-temperature pipe along the length of the pipe. The pressure losses along these holes result in a linear relationship between motor power and ball distance. Thus, with this prototype, the ball distance could now be controlled with the help of a PID controller.

4. The mass product

While the first prototype represented a good milestone and proof of concept, it could not be manufactured in a high quantity, since, for example, removing the fans from 400 hair dryers is not economically or logistically feasible. In addition, the provisional mount made of cardboard boxes ought to be replaced by a more stable structure and a light barrier to be added to the setup to enable accurate load shedding tests. PC fans came forward as a replacement for the hair dryer fans, since they have a standardized size with a hole pattern, which simplifies the development of a mount. However, a high maximum airflow of the fans was required compared to normal use, while noise generation could be neglected. This significantly limited the models that could be used. For the production of the mount, various manufacturing methods were found unsuitable, since, for example, 3D printing and the milling of many parts would have involved long manufacturing times and high personnel costs. However, high-output methods, such as injection molding, were also ruled out due to the finite number of pieces. Therefore, threaded rods, laser-cut steel plates and nuts were used to take advantage of the hole profile of the fans to obtain a stable experimental setup, as shown in Fig. 4.

The high-temperature pipe was replaced by a Plexiglas pipe, which makes the experiment much more vivid due to its transparency. Instead of holes, slots were milled in the sides and another opening at the bottom of the pipe.

An orifice can be inserted here to restrict the air flow and is registered electronically by a light barrier. In addition, a bridge for the ultrasonic sensor was glued on. The production of

the pipes required a large part of the manufacturing time due to the complex manual procedures involved. The potentiometer for changing the setpoint is no longer required, as this is now changed purely via the software.

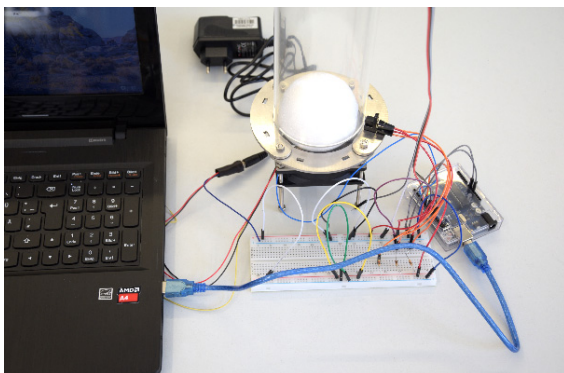


Fig. 4: From top to bottom. Upper end of the Plexiglas pipe with ultrasonic sensor. Lower experimental setup consisting of fan, threaded rods, nuts and laser-cut steel plates. Fully wired experimental setup.

5. The do-it-yourself variant

For those who could not get access to experimental suit cases, a special instruction was created describing an alternative experimental setup. This represents a mixture of the first prototype and the experimental setup given out at the end. The materials for this must be organized independently.



Fig. 5: Student's setup from a high-temperature pipe and clamping components [3.]

The same electrical components are used, but a high-temperature pipe or a cardboard pipe with a hole pattern is used as a controlled system, to which the fan is attached with adhesive tape. Cardboard boxes or books are suggested as mounts. In general, improvisation and personal engineering solutions were allowed here.

An outstanding student's setup using building blocks and a high-temperature pipe about one meter long is shown in Fig. 5 shown. A detailed view of the base is shown in Fig. 6. Because of the pipe length, the beam angle of the ultrasonic sensor was reduced to increase the

range of the sensor, as shown in Fig. 7. This example shows that very creative and sophisticated solutions can be stimulated with the help of the experimental and special instructions.

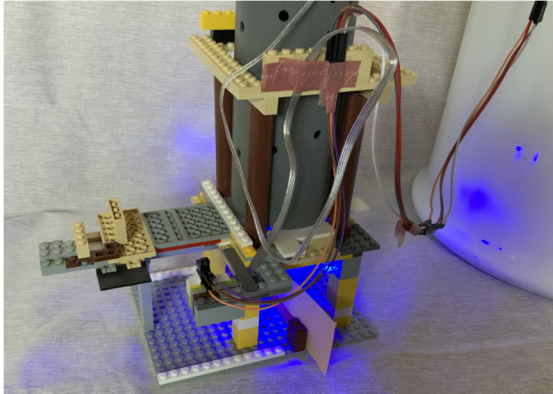


Fig. 6: Detailed view of the lower base [3].



Fig. 7: Ultrasonic sensor with reduced beam angle for range extension [3.]

6. The didactic concept

Since system responses are now also handled by other experiments, the focus of the new control loop experiment should rather be on controllers in general and the PID controller and its setting in particular. Programs for the Arduino are provided by the chair for all tasks. Individual programming knowledge is not necessary for the execution of the experiment in advance, but the logic of the programs used must be understood so that small changes can be made, such as the insertion of numerical values. First, the controlled system must be characterized. For this, different powers of the fan are set, and the heights reached by the Styrofoam ball are measured. The relationship

is then shown in a diagram. From the values determined, the operating range of the controller and important parameters for the further experiments are obtained, which must be noted. Now a simple two-point controller is measured and extended by a hysteresis. The measured curves are again to be displayed in a diagram and the frequency and amplitude of the oscillations are to be determined. As a transition from the two-point controller to the PID controller, a pure P controller is now used, whose three limiting cases of a subcritical, critical and supercritical controller gain are investigated. A presentation with diagrams is made to compare the cases. According to Ziegler and Nichols, the critical behavior can be used to determine the controller parameters of a PID controller, which will be used for the next experiment [4]. The self-determined PID controller is now characterized by recording a step response and load shedding of the system, plotting it and evaluating it using common criteria. An alternative method of determining parameters is shown by recording an uncontrolled step response of the system and determining proportionality and time constants from this system response, which allow PID parameters to be determined using the lambda method [5]. These settings will also be tested using controlled step response and load shedding. Lastly, the two controllers created according to Ziegler and Nichols and according to Lambda will be compared and discussed. Optional tasks, such as the variation of the hysteresis in the case of the two-point controller or the optimization of the controller parameters are an opportunity to familiarise oneself with controllers even more, depending on the individual interest.

7. The correction

Since approximately 500 persons participate in the practical course and approximately 250 protocols have to be corrected due to groups of two, the correction should be made as simple and time-effective as possible in order to minimize the time burden on the staff of the chair. Therefore, a high focus is put on diagrams in the tasks, because they straightforwardly point the correct execution of the experiment to the supervisors. A sample proto-

col was given in which diagrams and measured values had to be entered at corresponding placeholders. Open questions were only asked in a few places in order to avoid lengthy texts with higher correction effort.

8. The test

In the following the experiment is tested in detail, whereas the procedure used for this is beyond what is expected and required in the student execution of the practical course. The Arduino programs provided to the students were modified so that during a measurement the parameters are automatically changed incrementally according to time intervals, which allows fully automatic data recording with the exception of load shedding. The evaluation was performed via a Python script.

The characterization

To characterize the controlled system, the PWM value used to adjust the fan power was increased from 120 to 255 in increments of 2.5 every 30s. The mean values and the twofold standard deviation were determined for the ball distance d while the data for the first 10s per PWM value were discarded to consider only the equilibrium condition. The variation of the ball height h for the different PWM values is shown in Fig. 8. Initially, the ball remains at rest until it begins to float at PWM_{min} and above. The ball increases relatively linearly with the PWM-value until the upper end of the pipe is reached. Since the slots are not continuous, a more complex oscillating floating behavior of the ball occurs here, since the flow is dependent on the ball position itself. At higher PWM-value, the ball is pressed towards the ultrasonic sensor and falls below the minimum distance of the sensor. This leads to strongly fluctuating measurement results of the sensor. At even higher PWM-values this behavior does not change. PWM_{max} now represents the maximum PWM-value at which the ball still floats stable and does not fall below the minimum distance of the sensor. The change of the measurement fluctuation can be used as a determination criterion for PWM_{max} . The value of PWM_{max} is thus the highest PWM value at which there is still a significant distance, i.e. it is greater than its twofold standard deviation d :

$$d > 2\sigma_d \tag{1}$$

The values of d_{max} and PWM_{min} were determined iteratively. First, the distance at the lowest PWM-value was taken as the maximum distance d_{max} and the ball height h was calculated from the difference:

$$h = d_{max} - d \tag{2}$$

For PWM_{min} , the first PWM value at which there was significant ball hovering was used:

$$h > 2\sigma_d \tag{3}$$

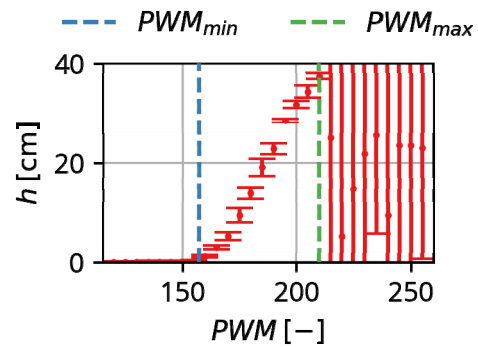


Fig. 8: Characterization of the controlled system. Plotted is the ball height against the used PWM-values.

| Tab. 1: Values determined from the characterization. | |
|--|---------------------|
| d_{max} | $(43,3 \pm 0,1)$ cm |
| $2\sigma_d$ | 1,2 cm |
| PWM_{min} | 157,5 |
| PWM_{max} | 210 |

Subsequently, d_{max} was calculated as the mean value of all values $PWM < PWM_{min}$ and the procedure was carried out again until convergence. In addition, the mean variation $2\sigma_d$ for all d from PWM_{min} to PWM_{max} was determined. This is an indicator of how stable the setup is without a controller. The determined values are summarized in Tab. 1.

The two-point controller

Subsequently, a two-point controller with the determined values PWM_{min} and PWM_{max} and different hysteresis widths d_H was tested. For this purpose, values for 30 s per each d_H were recorded and were ranged from $d_H = 0$ cm to $d_H = 24$ cm in steps of 4 cm. The time curve of h and the PWM-values for $d_H = 0$ cm is shown

in Fig. 9 is shown. The ball height shows a harmonic oscillation, while the PWM values show a square wave.

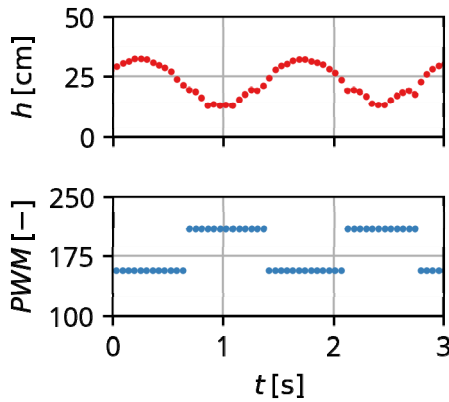


Fig. 9: Temporal progression of the height and PWM values for a two-point controller without hysteresis.

For the evaluation of the hysteresis influence, the frequency and amplitude of the oscillations were determined. Here, the first 10 s per d_H were discarded in order to consider only the equilibrium state. First, the difference of an oscillation to its mean value was formed and the zero points were determined, with a filter reducing closely spaced zero points caused by signal noise to a single zero point.

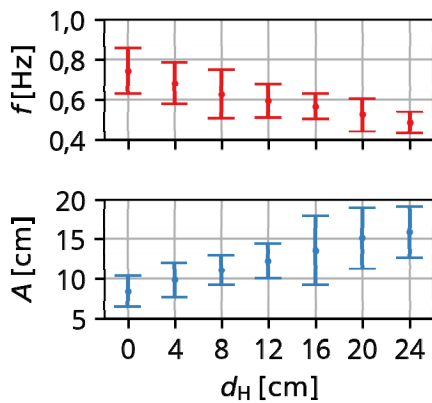


Fig. 10: Frequency and amplitude of the two-point controllers with increasing hysteresis width.

The period was determined by taking twice the mean temporal difference of the zero points and the frequency as the reciprocal. The mean values of the maximum amplitude between the zero points were determined as the amplitude of the oscillation. The frequencies and

amplitudes are plotted in Fig. 10 against the hysteresis width. The frequency decreases with d_H while the amplitude A increases.

The P controller

For the determination of the critical controller gain $K_{p,crit}$ first a pure proportional controller from $K_p = 1 \text{ cm}^{-1}$ to $K_p = 15 \text{ cm}^{-1}$ was tested and it was visually determined when an oscillation approximately starts. Subsequently, a series of measurements from $K_p = 2,5 \text{ cm}^{-1}$ to $K_p = 5 \text{ cm}^{-1}$ in steps of $0,1 \text{ cm}^{-1}$ with each 30 s per K_p -value was performed. For the evaluation, the first 10 s per K_p -value were discarded to avoid effects from transient behavior.

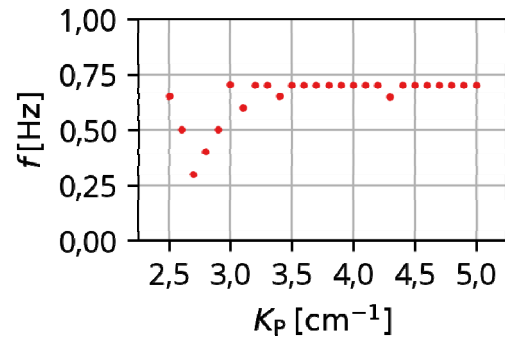


Fig. 11: Frequencies each with the maximum amplitude from the Fourier transform for pure P controllers over different values of K_p .

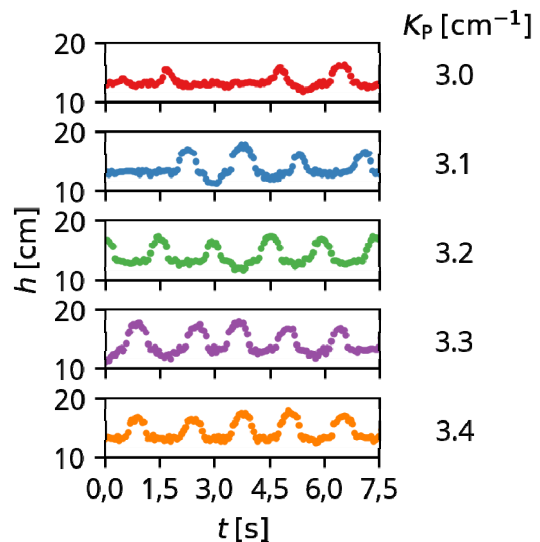


Fig. 12: Temporal progression of the height of a P controller with $K_p = 3,0 \text{ cm}^{-1}$ to $K_p = 3,4 \text{ cm}^{-1}$.

For each K_p -value, a Fourier transform was performed and the frequency with the largest

amplitude in the frequency spectrum was determined. The determined dominant frequencies are shown in Fig. 11. For K_p -values above 3 mm^{-1} a frequency of about $0,7 \text{ Hz}$ stands out, while at low K_p -values, especially when looking at the frequency spectra themselves, rather random frequencies are present.

For a more precise determination, the curve progressions in the range from $K_p = 3,0 \text{ cm}^{-1}$ to $K_p = 3,4 \text{ cm}^{-1}$ are considered, as shown in **Fehler! Verweisquelle konnte nicht gefunden werden..** Here it can be seen that a stable harmonic oscillation only starts with $K_{p,Krit} = 3,2 \text{ cm}^{-1}$. The period duration is $T_{Krit} = 1,46 \text{ s}$.

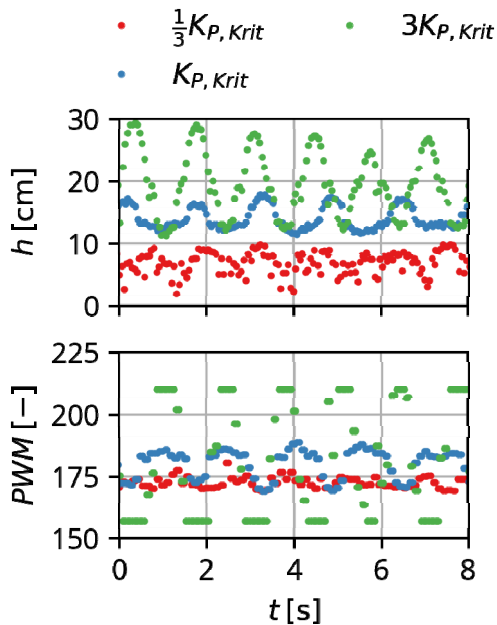


Fig. 13: Temporal progression of the height and the PWM-values of P controllers with subcritical, critical and supercritical controller gain.

To illustrate the P controller, controllers with subcritical, critical and supercritical controller gain were now tested. The time curves of h and PWM are shown in Fig. 13. For the subcritical behavior, both h , as well as PWM are nearly constant, with minor fluctuations occurring. In the case of critical behavior, these both form a harmonic oscillation, whereby these are shifted by 180° out of phase. The phase shift results from the calculation of h . For the supercritical behavior the mean height, as well as the amplitude of the oscillation increases. For the

PWM -values, a transition from a harmonic oscillation to a rectangular oscillation becomes apparent.

The Ziegler-Nichols setting

With $K_{p,Krit}$ and T_{Krit} the controller parameters according to Ziegler and Nichols can be determined. The parameters are listed in Tab. 2. With the controller parameters set, three step responses were now carried out by changing the setpoint value d_s from 35 cm to 15 cm .

| | |
|---|---------------------------------------|
| $K_{p,Krit}$ | $3,2 \text{ cm}^{-1}$ |
| T_{Krit} | $1,46 \text{ s}$ |
| $K_p = 0,6 K_{p,Krit}$ | $1,92 \text{ cm}^{-1}$ |
| $K_I = 1,2 \frac{K_{p,Krit}}{T_{Krit}}$ | $2,69 \text{ cm}^{-1} \text{ s}^{-1}$ |
| $K_D = 0,075 K_{p,Krit} \cdot T_{Krit}$ | $0,34 \text{ cm}^{-1} \text{ s}$ |

The following parameters are determined for evaluation:

- σ_s , the standard deviation in the controlled state after the step in the equilibrium state.
- x_{os} , the relative height of the maximum overshoot, normalized to the setpoint value
- t_1 , the time after which the $\pm 7,5\%$ -band of the set point is reached for the first time.
- t_2 , the time after which the $\pm 7,5\%$ -band is kept at all times

The curves and mean values of the parameters are shown in Fig. 14. The step responses are quite reproducible in their dynamics despite fluctuations before the step. The parameters with statistical uncertainties are listed in Tab. 3. The shape is characterized by an overshoot of $14,1 \%$ with a characteristic exponential decrease of the oscillation. The ball reaches the $\pm 7,5 \%$ -band after 732 ms and stays within it at all times after 1390 ms . A metal shutter was used to throttle the airflow and load shedding was performed by pulling the shutter. For evaluation σ_s , x_{os} and t_1 are determined, where t_1 represents the time from which, after the overshoot, the $\pm 7,5 \%$ -band is reached again for the first time. The curves and mean values of

the characteristics are shown in Fig. 15. In the curves, there is initially an overshoot of 49,1 %. The ball reaches the $\pm 7.5\%$ -band after 1200 ms but a relatively strong oscillation occurs afterwards, which leaves the $\pm 7.5\%$ -band several times. This oscillation does not decrease with time. The determined parameters with statistical uncertainties are listed in Tab. 4.

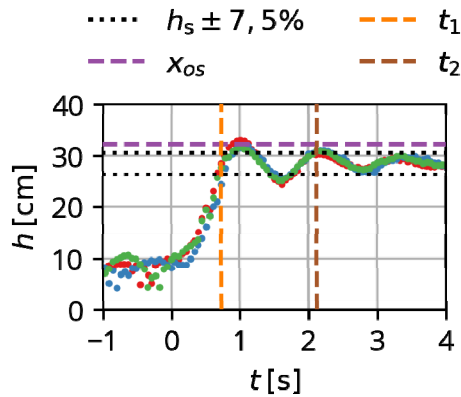


Fig. 14: Temporal progressions of three step responses and the mean values of the characteristic parameters for the controller according to Ziegler and Nichols.

| | |
|------------|---------------------|
| σ_s | $(1,6 \pm 0,1)$ cm |
| x_{os} | $(14,1 \pm 3,7)$ % |
| t_1 | (732 ± 92) ms |
| t_2 | (1390 ± 470) ms |

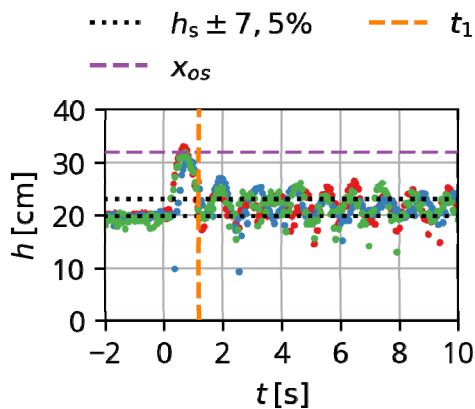


Fig. 15: Temporal progression of three load sheddings, as well as the mean values of the characteristic parameters for the controller according to Ziegler and Nichols.

| | |
|------------|---------------------|
| σ_s | $(7,4 \pm 2,2)$ cm |
| x_{os} | $(49,1 \pm 9,3)$ % |
| t_1 | (1200 ± 140) ms |

The lambda setting

In addition to the critical method, the controlled system can be characterized by means of an uncontrolled step response, where the specified PWM-value is changed. Three step tests are shown in Fig. 16.

The following parameters are determined for the characterization:

- $K' = \frac{\Delta h}{\Delta PWM}$ the quotient of the output and input value change
- t_t the delay time of the system until there is a significant change from h
- τ the time needed after the delay time until $0,63\Delta h$ is reached

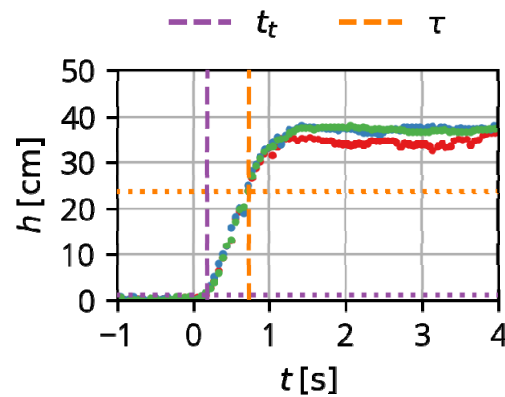


Fig. 16: Temporal progression of three uncontrolled step responses to characterize the controlled system.

The controller parameters can be determined from these values according to the lambda setting. The values and parameters are listed in Tab. 5. For the calculation of K_C a $N = 3$ was chosen, which should lead to a slow but stable controller. As with the Ziegler-Nichols setting, the controller is tested with a jump test and a load shedding. The curves of the step response tests are shown in Fig. 17 and their step responses are listed in Tab. 6.

Compared to the Ziegler-Nichols setting, the controller is much slower. The $\pm 7.5\%$ -band is reached only after 2560 ms which corresponds

Tab. 5: Values from the uncontrolled step response and controller parameters after lambda adjustment.

| | |
|--------------------------------------|-------------------------------------|
| K' | $(0.69 \pm 0,02) \text{ cm}$ |
| t_t | $(187 \pm 26) \text{ ms}$ |
| τ | $(551 \pm 46) \text{ ms}$ |
| $K_C = \frac{\tau}{K'(N\tau + t_t)}$ | $0,43 \text{ cm}^{-1}$ |
| $K_p = K_C$ | $0,43 \text{ cm}^{-1}$ |
| $K_I = \frac{K_C}{\tau}$ | $0,78 \text{ cm}^{-1}\text{s}^{-1}$ |
| $K_D = 0$ | $0 \text{ cm}^{-1}\text{s}$ |

fields of application. Parameters according to Ziegler and Nichols are easier to determine and a faster controller is obtained. However, this requires a robust system which is not damaged by oscillation or overshoots. With the Lambda settings, on the other hand, overshoot can be avoided. However, the determination procedure is more complicated and the controller is slower and more sensitive to disturbances. In general, the determination methods shown are rather the starting points for a manual optimization of the controller parameters for a specific application.

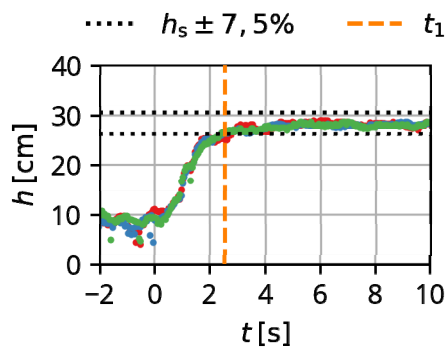


Fig. 17: Temporal progression of three step responses and the mean values of the parameters for the lambda setting.

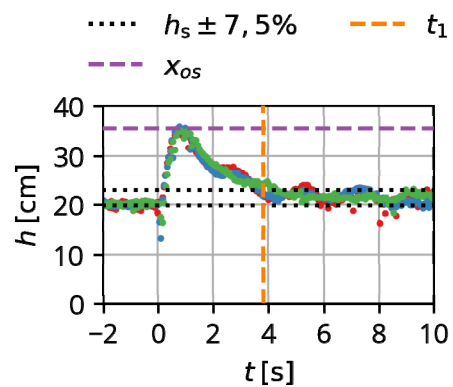


Fig. 18: Temporal progression of three load shedding events and the mean values of the parameters for the lambda setting.

Tab. 6: Evaluation of the step test for the lambda setting.

| | |
|------------|-----------------------------|
| σ_s | $(1,3 \pm 0,2) \text{ cm}$ |
| x_{os} | $(0 \pm 0) \%$ |
| t_1 | $(2560 \pm 340) \text{ ms}$ |
| t_2 | $(0 \pm 0) \text{ ms}$ |

Tab. 7: Evaluation of the load shedding for the lambda setting.

| | |
|------------|-----------------------------|
| σ_s | $(3,7 \pm 0,3) \text{ cm}$ |
| x_{os} | $(66,3 \pm 1,4) \%$ |
| t_1 | $(3840 \pm 670) \text{ ms}$ |

to three and a half times the duration of the Ziegler-Nichols setting, but is not left afterwards at any time. In addition, there is no overshoot and the oscillation in the equilibrium state is smaller. The curves of the load shedding are shown in Fig. 18 and their parameters are listed in Tab. 7. The load shedding shows a slightly higher overshoot of 66,3% and it takes 3840 ms until the setpoint is reached again. On the other hand, the oscillation after load shedding is only about half as large as the one observed with Ziegler and Nichols. The Lambda setting is therefore slower and more susceptible to external disturbances, but avoids overshoots when reaching a setpoint and is then more stable. The two methods have different

9. The student implementation

The lab course was carried out in the summer semester of 2021. Findings from this performance as well as findings from the experiment described here were used to revise the instructions and the tasks, whereby differences to our own experiment will be explained in more detail below. The students are in the 6th semester when carrying out the experiment, so that deeper programming knowledge such as the use of program loops cannot be assumed. Instead, the intention is to experiment with the programs provided by manually editing the numerical values and observing their effect on the experimental setup. First experiences with

an Arduino will be acquired in other previous experiments. While with program loops the possible power range of the fan can be fully observed automatically, simply running such programs would not be very interactive and would not lead to much involvement of the participants. By varying the values manually, the characterization of the controlled system has an exploratory character and considerations have to be made about the reasonable distribution of the measurement points to fulfill the task. Thus, in the vicinity of PWM_{min} or PWM_{max} higher measuring point densities may be considered, while a lower density is sufficient for the linear range in between. Due to the time frame of the experiment, only an introduction of a hysteresis was required in the case of the two-point controller, but not the variation of the hysteresis width, as it was done here. As an optional task, however, a further hysteresis width can be tested out. In a group of participants as a sample ($N = 29$) an average of 55 % of the points of this optional task were achieved. As in the case of the characterization of the controlled system, $K_{p,Krit}$ could be determined by a program loop, but the manual determination trains the estimation of and approximation to values. In addition, no handling of Fourier transforms, as it was exercised here, can be expected, so that instead a keen observation is more important. An obstacle here, however, was the transient process, since this allows an oscillation to be observed, which decays over time. As a result, lower $K_{p,Krit}$ were determined in the student execution in general. After a revision of the instructions, explicit reference is now made to the transient response. Originally, for step response and load shedding a $\pm 5\%$ -band was suggested, but it became apparent, especially with the Ziegler-Nichols setting, that this, depending on the choice of $K_{p,Krit}$ is too small of a tolerance band, so that now generally a $\pm 7,5\%$ -band is suggested for the test. In some cases, Ziegler-Nichols settings showed a very unstable behavior when a too high $K_{p,Krit}$ was used by the students. The evaluation of the data and the creation of diagrams were carried out in the student evaluation with the aid of spreadsheet programs in general and in exceptional cases with Matlab. The optimization of a controller represented a further optional

task, while in the sample on average only 25 % of these points were achieved. However, compared to the other optional task, this task also represents a considerable additional effort. Overall, with 83 % of the points to be achieved in the sample, the tasks were well fulfilled by the participants, with about 6 % of these points coming from the optional task parts. The issuing and return of the experimental suite cases took place without major difficulties. Grades were not recorded until the experimental kit was returned in its entirety. About 10 Arduinos had to be replaced, while defects may have already existed at the factory level, since for time reasons not all Arduinos could be tested prior to issuing. On the other hand the plugging of the 12 V fan power supply to the 5 V input of the Arduino is another possible cause. In the instructions it is now explicitly pointed out not to do this.

10. The conclusion

With the control loop experiment shown here, an old experiment of the chair was redeveloped. Due to the change of the medium, the experiments can be carried out more quickly. With the exception of the pipe, the experiment is very compact and part of the experimental case of the chair. The special instructions make it possible to set up an equivalent setup with one's own materials and carry out the experiment even without the experimental kit. From a didactic point of view, the students are led from a simple two-point controller via a P-controller to a PID-controller and learn about the characterization and various setting rules of these controllers. As can be seen from the results shown here, very different controllers can be well illustrated with this setup. In the MAT practical course of the summer semester 2021, the experiment was successfully carried out with 400 students, and findings from this implementation were incorporated into a revision of the instructions and task definition. The exact measured values of a setup can vary depending on the fan and the quality of the setup, such as the inclination of the pipe, so that each student group has a setup with individual values.

Acknowledgement

We would like to thank the FOSTER program of the TU Dresden for the financial support of the project. In addition, we would like to thank employees of the Chair of Magnetofluid Dynamics, Measurement and Automation Technology, who constructively contributed to the development of the experiment as beta testers, as well as Lars Gladrow and the employees of the workshop and experimental field group for the considerable manpower required for the production of the test stands. Thanks to Karl Kaden and Kevin Klinkicht for the use of the photos of their setup.

Literature

- [1] S. Odenbach, L. Selzer, and J. Morich, "Internship without presence - is it possible?," *Lessons Learned*, no. 1, pp. 1-2, 21 07 2021.
- [2] B. Beauregard, "Arduino PID Library," [Online]. Available: <https://github.com/br3ttb/Arduino-PID-Library>.
- [3] Photos: K. Kaden and K. Klinkicht. Private correspondence
- [4] Ziegler J.G. and Nichols N.B., Optimum settings for automatic controllers, *Trans. ASME*, pp. 759-768, 1942
- [5] Dahlin E.B., Designing and Tuning Digital Controllers, *Instr and Cont Syst*, 41 (6), 77, 1968.